Comparative Performance of a Substandard Beam-Column Joint with and Without Initial Bond Between Beam Bars and Concrete in the Joint Core

Teeraphot Supaviriyakit
Graduate student, Sirindhorn International Institute of Technology,
Thammasat University, Pathum Thani, Thailand,
teeraphot@hotmail.com
Amorn Pimanmas
Associate Professor, Sirindhorn International Institute of Technology,
Thammasat University, Pathum Thani,
Thailand, amorn@siit.tu.ac.th

Abstract

This paper presents the test of a beam-column joint with and without bond between concrete and longitudinal bar in the joint. The specimens are half-scale, typical of substandard actual beam-column joint of mid-rise reinforced concrete frame buildings constructed in Thailand. In Thailand, the design and construction of RC frames do not normally take into account the seismic loading. For the control specimen with full bonding, the failure was suddenly caused by crushing of a concrete strut. The energy was dissipated through diagonal cracks in the joint. On the contrary, for the specimen with debonded longitudinal reinforcement, little damage was observed in the joint. The joint remained sound throughout the entire loading. The deformation was concentrated as a fixed end rotation around the interface between the joint face and beam. As a result, the energy was mainly dissipated at the interface rather than at the joint. Either mode of failure was undesirable in terms of energy dissipation. However, the drop in load after peak of the debond specimen was more gradual than the abrupt crushing observed in the control specimen. The experiment shows the significance of the bond on the failure mode of reinforced concrete beam-column joints.

Keywords : Beam-column joint, Bond deterioration, Debond, Reversed cyclic loading, Joint shear

1. Introduction

The lateral resistance of a rigid frame is derived from bending in beams and columns. Under lateral load, a beam-column joint has to transfer unbalanced moment between the beam and columns. This creates horizontal shear forces in the joint as shown in **Fig.1**. This joint shear force is found to be several times greater than shear forces in beams and columns [1, 2]. Obviously, the beam-column joint is one of the most critical components in the lateral load path of a frame. In Thailand, the design of reinforced concrete frame buildings normally considers the gravity load only according to the ACI building code (ACI318) [3]. Hence, the member design and reinforcement detail do not meet the modern practice of seismic ductile reinforcement detailing. Particularly, the beam-column joints in these buildings lack confining stirrups and the size of a column is usually small.

The resultant forces in **Fig. 1** indicate that the joint shear force is transferred through a diagonal strut. The crushing of this strut

determines the joint shear failure. Moreover, the longitudinal beam reinforcing bar is subject to compression on one side and tension on the opposite side. This causes a significant bond force transfer between the concrete and longitudinal steel. The loss of bond changes the compressive stress in steel to tensile stress [4, 5]. As a result, the compressive force is increased to equilibrate the increased tension. Hence, it leads to a question whether the bond deterioration accelerates the crushing of the diagonal concrete strut. This paper attempts to investigate this problem by testing a beam-column joint with completely no bond between longitudinal bar and concrete in the joint. The result is compared with the control specimen where full bonding is provided. Another objective is to study the performance of substandard interior beam-column connection constructed in Thailand.

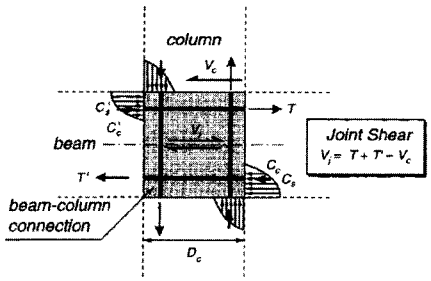

Figure 1 Joint shear force

2. Experimental Program

2.1 Specimen

The experiment was conducted to study the bond between beam longitudinal reinforcement and concrete in a substandard interior beam-column joint. The authors tested two beam-column specimens, a control and a debond specimen. The beam-column specimen was half-scale, representing the typical beam-column connection of mid-rise (6-15 storey) reinforced concrete frame buildings constructed in Thailand. The member size and reinforcement details (**Fig. 2**) of these two specimens were designed to closely match the average of the database of actual reinforced concrete frame building studied by Warnitchai [6] and Chaimahawan and Pimanmas [7]. The comparison of various key structural parameters of actual buildings and specimen is given in Table 1.

Note : BI = bond index = $f_y d_b / 2h_c\sqrt{f_c'}$, h_c = column depth (in the direction of loading), h_b = beam depth, d_b = diameter of longitudinal bar, b_b = width of beam, b_c width of column (orthogonal to h_c), M_{nc} = nominal moment capacity of column, M_{nb} = nominal moment capacity of beam, V = joint shear force, V_n = joint shear capacity, ρ_s = volumetric ratio of joint transverse reinforcement.

The size of beam was 175 mm x 300 mm and the size of column was 200 mm x 350 mm. The beam longitudinal reinforcements consisted of 6 DB12 (12-mm diameter deformed bar) top bars, and 4 DB12 bottom bars. The beam stirrup was 3 RB3@100 (3-mm diameter plain round bar). The column longitudinal reinforcement consisted of 18 DB12 and the stirrup was 3 RB3@100. The two specimens were identical except the bond condition of the longitudinal beam reinforcement passing through the joint core. In the debond specimen, the bond was initially removed completely by grinding the ribs of deformed bars, coating the surface with grease and wrapping the bar with plastic sheet

2.2 Material properties

The tested material properties are given in Tables 2 and 3 for the concrete and reinforcing bars, respectively.

2.3 Test set-up, instrumentation and load history

The experimental set-up is shown in **Fig. 3**. Both ends of the beam were supported by rollers that allowed horizontal movement to simulate lateral drift. The bottom end of the column was pinned to the base. The load was applied by a hydraulic actuator at the top of the column. The actuator was reacted against a 500 kN reaction frame fixed to a strong floor. In order to simulate the axial force on the column, prestressing tendons were provided in the column to supply an axial force of 300 kN. Figure 4 shows a photo of the specimen set-up in the laboratory. The instrumentation consisted of 1) horizontal force measurement and horizontal displacement, 2) flexural rotation in beam and column, 3) shear deformation in beam, column and joint, 4) rocking angle at the interface between joint face and beam, 5) strains of longitudinal steel and stirrup in beam and column.

Table 1 Structural index for beam-column joint

Parameter / Statistical value	BI	$\frac{h_c}{d_b}$	$\frac{b_b}{b_c}$	$\frac{h_b}{h_c}$	$\frac{M_{nc}}{M_{nb}}$	$\frac{V}{V_n}$	ρ_s
Maximum	6.19	60	1.00	1.08	3.40	1.524	0
Minimum	2.24	24	0.50	0.63	1.54	0.912	0
Average	4.51	37	0.80	0.84	2.36	1.254	0
Standard deviation	1.65	16	0.12	0.23	0.78	0.113	0
Specimen	5.09	29	0.88	0.86	1.68	1.382	0

Table 2 Tested properties of concrete (MPa)

Compressive strength, fc′(MPa)	Control Specimen	Debond Specimen
Top column	23.7	26.8
Beam	26.8	21.7
Bottom column	23.2	25.0

Table 3 Tested properties of longitudinal steel and stirrup

Properties	Longitudinal steel (12-mm dia. Deformed bar)	Stirrup (3-mm dia. Round bar)
Yield Strength (MPa)	488.6	312.0
Tensile Strength (MPa)	637.3	395.0
Modulus of elasticity (MPa)	2.04×10^5	2.04×10^5

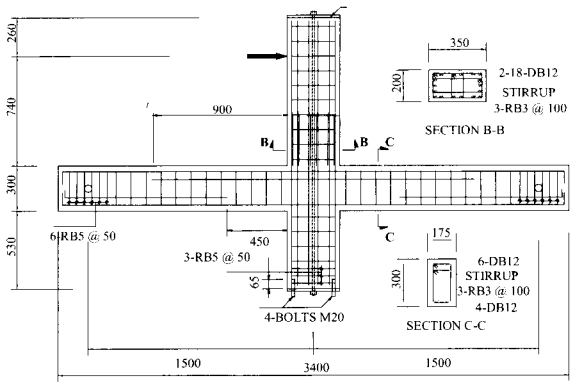

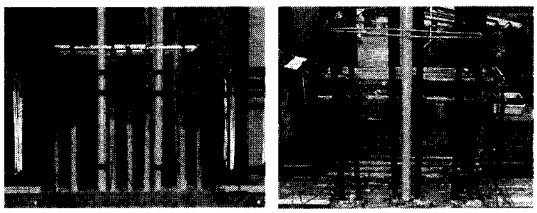

Control specimen Debond specimen

Figure 2 Specimen dimension and reinforcement detail

The load applied to the specimen was lateral cyclic displacement-controlled. The column was pushed and pulled with increasing interstory drift of ±0.25%, ±0.5%, ±0.75%, ±1% and so on as shown in Figure 5. At each drift level, the displacement was repeated twice to check the stability of the loop as well as to investigate the energy dissipation.

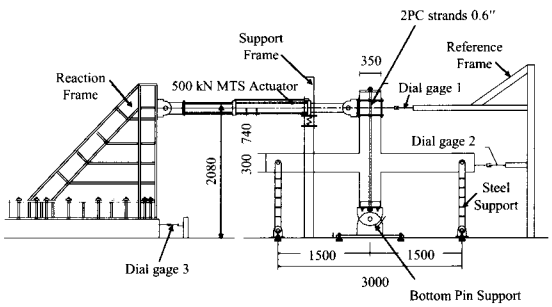

Figure 3 Test set-up

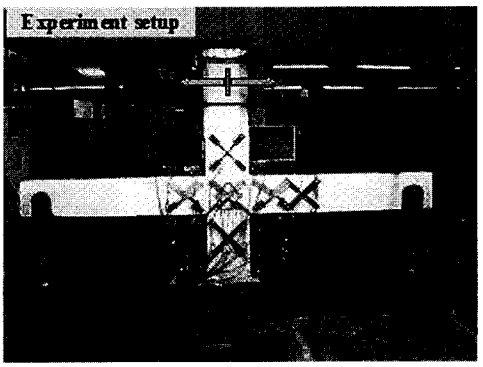

Figure 4 Photo of specimen set-up in laboratory

3. Experimental results

Table 4 gives an overall summary of experimental results. First, it is seen that the control specimen had 16% greater strength than the debond specimen. The drift at peak load of the control specimen was also larger than that of the debond specimen. However, the remaining strength of the debond specimen was larger, indicating a more gentle drop in the load capacity. The failure mode was also different. The control specimen failed by joint shear failure while the debond specimen failed by beam splitting and bond pull-out failure. In the following sections, a detailed discussion shall be provided.

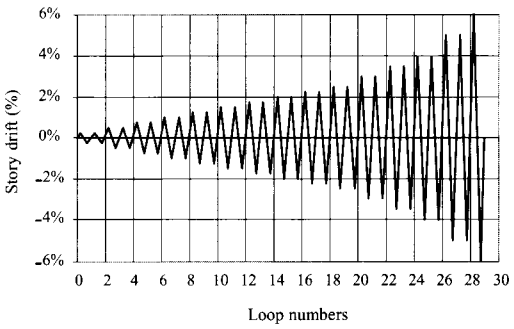

Figure 5 Load patterns

Table 4 Summary of test results.

Specimen	Peak point		Residual strength at 5% drift (as percentage of peak load)	Failure mode
	Force (kN)	Drift (%)		
Control specimen	72	1.75	44	Joint shear failure
Debond specimen	62	1.50	67	Beam splitting and Bond pull-out failure

3.1 General observation, cracking process and failure

(a) Control specimen

The cracking behavior of the control specimen is illustrated in **Fig. 6**. At ±0.25% drift ratio, flexural cracks developed as first cracks on the beam. At ±0.5% drift ratio, the first diagonal crack occurred at the joint. As the drift ratio increased, these flexural and diagonal cracks grew in size and numbers. At ±0.75% drift ratio, a splitting crack along the longitudinal beam bar in the joint was observed. After a ±1.0% drift ratio, the cracks were mainly concentrated in the joint region. These cracks were intersecting diagonal cracks with typical X-shaped pattern as shown in **Fig. 6**. On the other hand, no more flexural cracks were observed in the beam. The specimen reached a peak load of 72 kN at 1.75% drift. At ±2.0% drift ratio, the concrete in the joint region spalled off, exposing column longitudinal bars. The load was continued with significant damage concentrated in the joint region until ±5.0%.

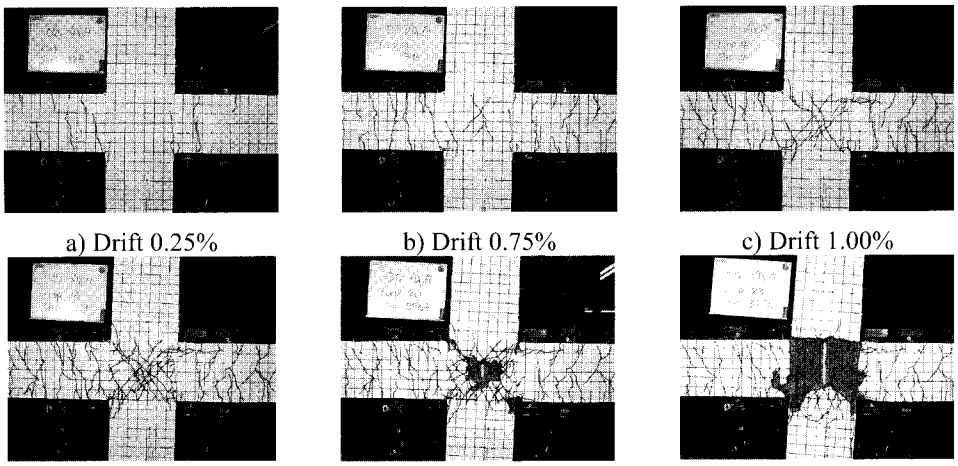

a) Drift 0.25% b) Drift 0.75% c) Drift 1.00%

d) Drift 1.75% e) Drift 3.0 % f) Drift 5.0%

Figure 6 Crack development in control specimen

(b) Debond specimen

The cracking behavior of the debond specimen is illustrated in **Fig. 7**. At ±0.25% drift ratio, a vertical crack was found at the interface between the joint face and beam. This crack indicated the pull-out slip of longitudinal beam bar. Flexural cracks were also observed in the beam but no diagonal crack occurred at the joint. As the drift increased, the pull-out crack widened. At ±1.0% drift, the first diagonal crack was observed in the joint. A horizontal splitting crack was also observed along the beam longitudinal bars. At ±1.25% drift, the interface pull-out crack as well as the beam splitting cracks widened substantially. The beam concrete cover spalled off. In contrast, the diagonal cracks in the joint were completely inactive, leaving the joint in a sound condition until as high as ±6.0% drift ratio.

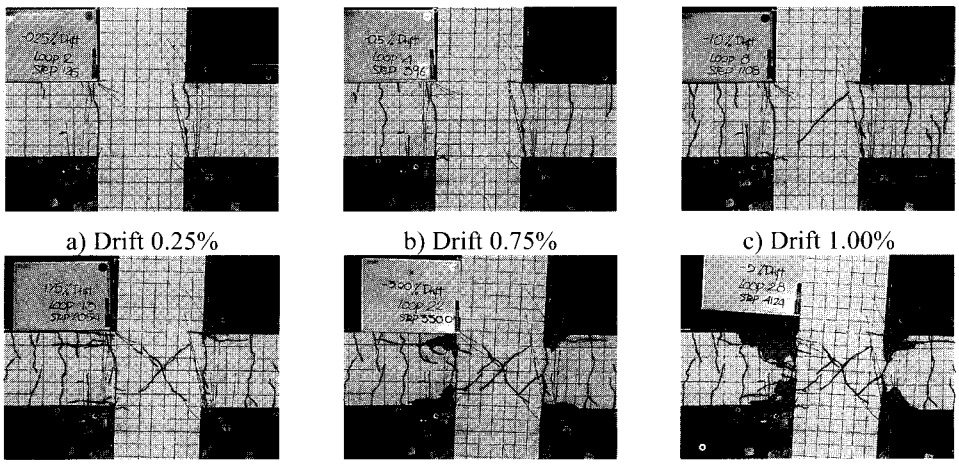

a) Drift 0.25% b) Drift 0.75% c) Drift 1.00%

d) Drift 1.75% e) Drift 3.0 % f) Drift 5.0%

Figure 7 Crack development in debond specimen

3.2 Story shear versus lateral drift relation

(a) Control specimen

The relation between story shear and lateral drift of the control specimen is shown in **Fig. 8**. As shown in the figure, the story shear-lateral drift relation of control specimen demonstrated elastic behavior within a lateral drift of ±0.50%. At ±0.75% drift, the hysteresis loops became pinched, indicating low energy dissipation upon cycling. The specimen began to yield at ±1.25% drift. It could resist the maximum story shear of 72 kN at 1.75% drift. Beyond 1.75% drift, the load dropped substantially. The failure behavior was brittle due to sudden crushing of the concrete strut. For any drift ratio after peak, the repeated cycle showed an obvious decrease in both strength and stiffness. The pinching in hysteresis loops became more evident, indicating a significant reduction of stiffness as a result of sliding of the diagonal crack in the joint. At 5% drift, the residual strength was 44% of the maximum load.

(b) Debond specimen

The story shear – lateral drift relation for the debond specimen is shown in **Fig. 9**. Elastic behavior was observed before ±0.50% drift, similar to the control specimen. Moreover, the hysteresis loops were narrow and pinched as a result of an opening of a pull-out crack at the interface. The specimen reached the peak load of 62 kN at 1.5% drift. However, the drop of peak load was not as sudden as that of the control specimen. It was supposed that the gradual reduction of peak load was caused by a gradual reduction of moment arm due to loss of the concrete compression zone on the beam's cross section. Similar to the control specimen, the repeated cycle at the drift beyond peak was unstable, and the loop was narrow with low energy dissipation. At 5% drift, the residual strength of specimen was 67% of the peak value.

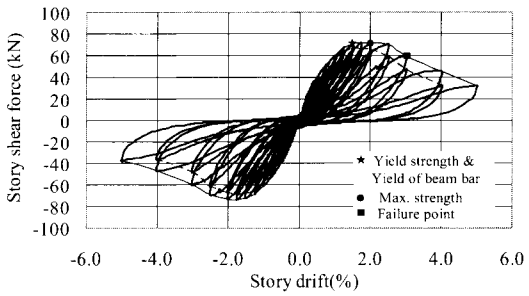

Figure 8 Story shear-story drift relation of the control specimen

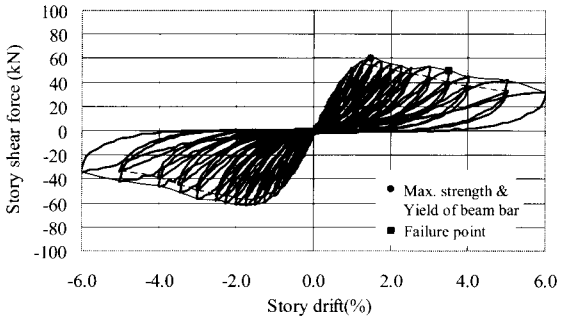

Figure 9 Story shear-story drift relation of the debond specimen

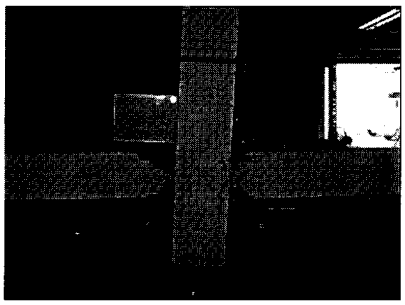

Figure 11 Tilting of column following spalling of beam concrete

3.3 Joint shear deformation-story drift relation

The relation between joint shear deformation and story drift is compared between the control and debond specimen as shown in **Fig. 10**. It is seen that the joint deformation of the debond specimen is substantially lower than that of the control specimen. This is because cracks and following nonlinearity are mainly concentrated around the beam ends due to a pull-out effect. As shown in the **Fig. 11**, the column of the debond specimen was displaced laterally while the beam remained straight. This suggests that a substantial rotation must occur at the beam-joint interface due to concrete spalling and bar pull-out. The total lateral top column displacement is compatible with this interface localized rotation while the joint deformation is very small. In contrast, diagonal cracks are mainly concentrated at the joint core of the control specimen, giving rise to significant damage of concrete core resisting diagonal compression. It may be concluded that the joint shear deformation causes the pinching characteristics in the control specimen while the interface localized rotation causes pinching in the debond specimen.

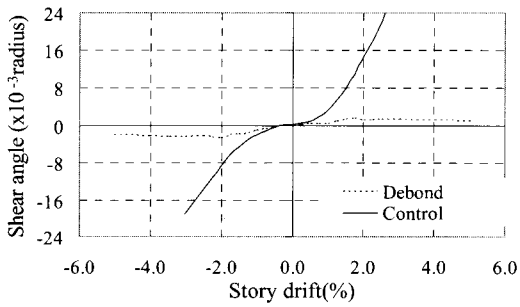

Figure 10 Comparison of joint shear angle-story drift relation

3.4 Analysis of longitudinal strains of beam bars

Fig. 12 shows the strain development at each load cycle of the control specimen. The strains are measured at beam longitudinal steel at 50 mm away from the column face. For the control specimen, the steel is tensile (positive strain) on one side and compressive (negative strain) on the opposite side in early drift levels. The magnitude of compressive strain is lower since the compression force is partly carried by concrete. As the drift increases, the compressive strain is gradually changed to tensile, indicating the bond deterioration. The envelope of strain is shown in **Fig. 13**. As shown, the strain reaches a yield strain at ±1.75% drift which is the peak load. After that, the strain drops. The strain drop is quite rapid even though significant bond deterioration does not yet take place. The drop in tensile strain is caused by a reduction of peak resistance due to joint crushing failure. **Fig. 14** shows the strain development at each load cycle of the debond specimen. It is seen that the specimen loses the bond from the beginning, hence, both steel sections are subject to a tension force even from the beginning of loading. Moreover, the strain in steels exceeds yield level as shown in the strain envelope in **Fig. 15**. This indicates the bars in the debond specimen maintain full yielding after peak resistance despite the nonexistence of bond in the joint. Hence, it is found that the steel could find the anchorage elsewhere even when no bonding exists in the joint core. As a result of high strains

in the beam close to the column interface, a splitting crack occurs and subsequently accelerates the concrete spalling. The reduction of peak resistance is caused by the loss of a concrete section, which leads to the movement of compressive resultant towards the beam mid-height and the reduction in the moment arm. This explains the drop in lateral load capacity of the specimen.

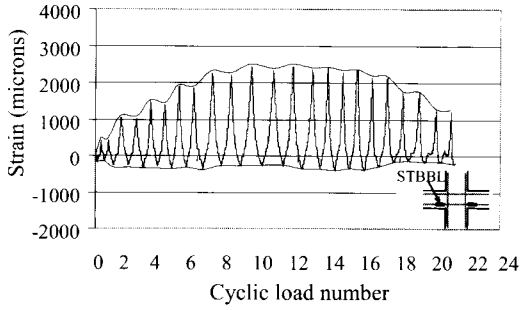

(a) Strain of beam bar at left side

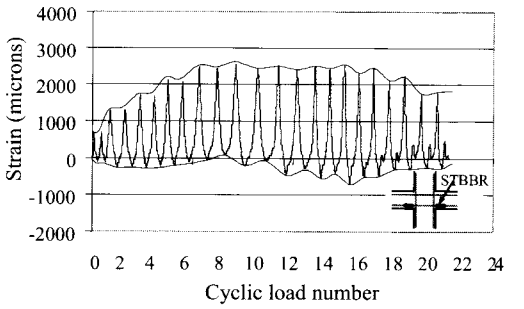

(b) Strain of beam bar at right side.

Figure 12 Strain of beam bar at any step of the control specimen

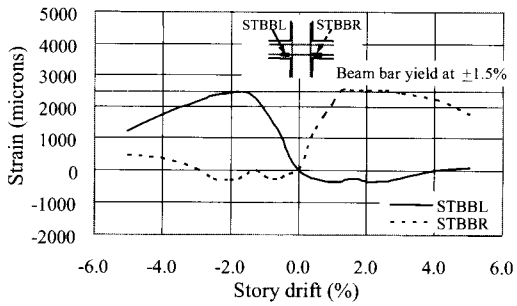

Figure 13 Strain envelope of the control specimen

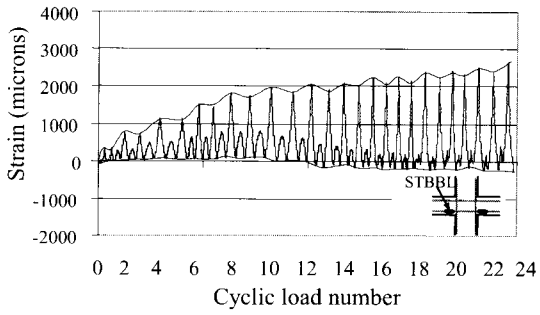

(a) Strain of beam bar at left side

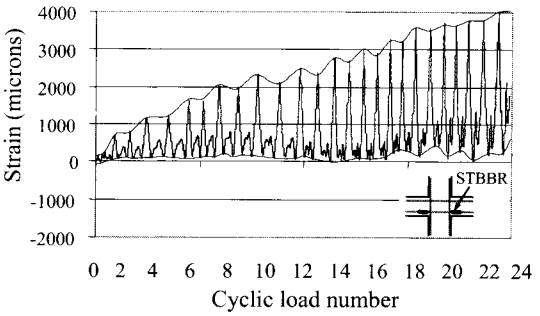

(b) Strain of beam bar at right side

Figure 14 Strain of beam bar at any step of the debond specimen

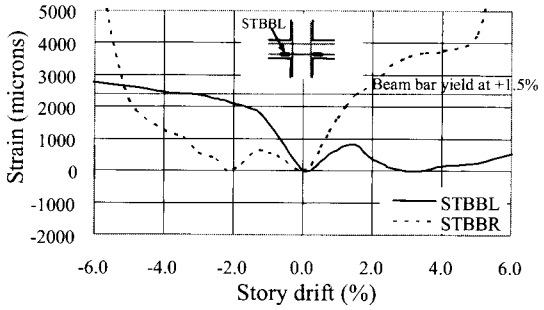

Figure 15 Strain envelope of the debond specimen

4. Failure mechanism and key structural parameters

The failure of specimens is discussed in connection with key structural parameters in this section. For the control specimen, the nominal moment capacity ratio of column to beam (M_{nc}/M_{nb}) was 1.63, which is greater than 1.2 as required by the ACI code. Hence, plastic hinge should form in the beam according to the weak beam strong column if joint failure is not premature. However, the ratio of joint shear to nominal joint shear capacity (V/V_n) is 1.38,

showing that the joint does not have sufficient capacity to resist shear. It should be recognized that the joint shear strength calculation is not required by ACI building codes for RC frame in low to moderate seismic zones. The ACI requires only minimum shear reinforcement to be provided in the joint core. In the control specimen, however, no stirrups are provided in the joint, causing the joint shear failure.

The bond index ($BI = f_y d_b / 2h_c\sqrt{f'_c}$) and the ratio of column depth to bar diameter (h_c/d_b) were 5.10 and 29, respectively. It is noted that no limitation of column depth to bar diameter is specified in ACI for an Intermediate Moment Resisting Frame (IMRF). For a Special moment resisting frame, the ACI sets the minimum column depth to bar diameter ratio at 20. It is found that the control specimen has not met the ACI requirement for IMRF. The specimen still showed brittle joint shear failure due to the lack of confining stirrups. In terms of bond behavior, the examination of strain of longitudinal beam bars also indicated certain bond deterioration of longitudinal bars.

As for the debond specimen, it is found that the majority of damage is concentrated in the beam close to the interface while very little damage occurs in the joint. From the strain analysis of longitudinal beam bar, it is found that steel is subject to tension on both sides of the joint in early load steps, as a result of no bond with concrete in the joint core. Hence, both top and bottom reinforcements are simultaneously subject to tension, and the concrete compressive force on the section must be doubled in order to maintain equilibrium. However, the horizontal joint shear is not correspondingly doubled. On the other hand, the horizontal shear remains almost unchanged. Figure 10 compares the horizontal joint shear under perfect bonding and debonding conditions. For perfect bonding condition, the horizontal joint shear is determined as (see Fig. 1):

$$V_j = T + T' - V_C \quad (1)$$

While for debonding condition, the equation may be written as (Fig. 16):

$$V_j = T + C' - T' - V_C \quad (2)$$

$$V_j = C' - V_C \quad \text{Since } T' = T \quad (3)$$

$$V_j = T + T' - V_C \quad \text{Since } C' = T + T' \quad (4)$$

The horizontal joint shear force should be recognized as a psudo joint shear force as it is computed from steel forces. The actual horizontal joint shear may be less if the beam concrete cover spalls off. This mechanism is shown in **Fig. 16**. In this case, the horizontal joint shear is determined from concrete compressive force rather steel forces as given below.

$$V_j = C'' - V_C \quad \text{where } C'' < C' \quad (5)$$

Where C'' is the resultant compressive force applied to the joint. Hence, it was seen that the actual joint shear force is less than the psudo joint shear force for the debond specimen. Moreover, from equation (4), it is seen that although debonding doubles compressive force, it does not change the psudo joint shear. From this analysis, it is therefore found that, the actual joint shear force is smaller than the psudo joint shear in the debond specimen. Consequently, joint shear damage and failure do not occur in the joint.

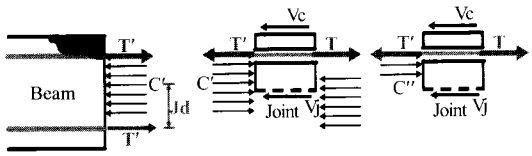

Figure 16 Actual horizontal joint shear for the debonding case with beam concrete cover spalled off

For the debond specimen, the beam splitting crack plays a major role on the failure behavior. The beam splitting crack causes the beam concrete cover to spall off and moves the compression resultant towards the midlevel of the beam. This causes a reduction in moment capacity of the section and hence, a story shear force. The movement of compression resultant on both sides of the joint made the strut inclination flatter, and hence, more effective to resist shear. Through this mechanism, the joint of the debond specimen remains sound

throughout the entire loading. The failure is determined by the localized interface pull-out behavior.

5. Conclusions

The test of a beam-column joint to identify the failure mode of substandard interior beam-column connection and the effect of bond between longitudinal bars and concrete is investigated in this paper. It is found that the control specimen with full bonding fails by the crushing of a diagonal strut in the joint region. The failure is brittle. The cause of failure is due to a high value of V/V_n and the lack of joint stirrups in the joint core. In contrast, the debond specimen fails by a bond pull-out failure with significant fixed end rotation at the interface between joint face and beam. The load drop after peak is more gradual than that of the control specimen. In terms of energy dissipation, either mode of failure was undesirable as the hysteresis loops are pinched with bad energy dissipation capacity. The beam splitting crack plays a major role on the failure behavior of the debond specimen. It causes spalling of the beam concrete cover, movement of compressive resultant towards midlevel, and increases the joint shear resistance through flatter geometry of diagonal strut. The debonding of longitudinal bars in the joint core does not affect the development of strain in the steel bar. The steel can find anchorage elsewhere and develops large plastic tensile strain even after peak. The psudo horizontal joint shear remains the same regardless of the bond condition. But the actual joint shear may be smaller under a debonding condition. As a result, the debonding reduces the joint shear damage which is beneficial in terms of post-earthquake retrofitting.

6. Reference

[1] Paulay T., and Priesley M.J.N., *Seismic Design of Reinforced Concrete and Masonry Buildings*. New York: John Wiley and Sons Inc., 1992.

[2] Kitayama, K., Otani S. and Aoyama, H., Development of Design Criteria for RC Interior Beam-Column Joints, *ACI SP-123, Design of Beam- Column Joints for Seismic Resistance*, pp.97-123, 1991.

[3] American Concrete Institute, *Building Code Requirements for Structural Concrete and Commentary*, Michigan, ACI committee 318, 2005.

[4] Shiohara H., New model for Shear Failure of RC Interior Beam-column Connections, ASCE J. Struct. Eng., Vol. 127, No.2, pp. 152-160, 2001.

[5] Hakuto S., Park R., and Tanaka, H., Effect of Deterioration of Bond of Beam Bars Passing through Interior Beam-column Joints on Flexural Strength and Ductility, ACI Struct. J. Vol.96 No.5, pp.858-864, 1999.

[6] Warnitchai P., Seismic Hazard Mitigation, Final Report Submitted to Thailand Research Fund (in Thai).

[7] Chaimahawan P. and Pimanmas A., Seismic Vulnerability of Existing Buildings in Bangkok, Proceeding of the 5th Int. Symposium for Urban Safety of Mega Cities in Asia, November 2006, Phuket, Thailand (CD-ROM).